Available online at www.sciencedirect.com
SCIENCE DIRECT®
Biochemical Pharmacology 65 (2003) 1061–1075
Biochemical Pharmacology
www.elsevier.com/locate/biochempharm

Cytotoxicity and apoptosis of benzoquinones: redox cycling, cytochrome *c* release, and BAD protein expression☆

Gabriela Tudor[a], Peter Gutierrez[b], Angelica Aguilera-Gutierrez[a], Edward A. Sausville[c,*]

[a]*Science Applications International Corporation, National Cancer Institute, P.O. Box B, Frederick, MD 21702, USA*
[b]*The University of Maryland Cancer Center, 655 W. Baltimore St., Baltimore, MD 21201, USA*
[c]*Developmental Therapeutics Program, DCTD, National Cancer Institute, EPN 8018, 6130 Executive Blvd., Rockville, MD 20852, USA*

Received 7 June 2002; accepted 14 August 2002

Abstract

The metabolic activation of a variety of quinone-based anticancer agents occurs, in part, as a result of the bioreductive activation by the flavoprotein NAD(P)H:quinone-acceptor oxidoreductase (NQO1) (EC 1.6.99.2). Using the COMPARE algorithm (http://dtp.nci.nih.gov), a significant statistical correlation has been found in the NCI *in vitro* anticancer drug screen between high endogenous expression of the pro-apoptotic protein BAD, NQO1 enzymatic activity, and the cytotoxicity of certain antitumor quinones. Two statistically correlated groups of quinones can be discerned: positive-correlated compounds, which are more active in cell lines expressing high baseline levels of BAD protein and NQO1 activity (e.g. the MCF-7 breast carcinoma), and negative-correlated compounds, which are more active in cell lines with undetectable levels of BAD and NQO1 activity (e.g. the HL-60 myeloid leukemia). In the present study, the relationship between quinone structure, redox cycling, and cytotoxicity in the MCF-7 and HL-60 cell lines was investigated. A good biological correlation exists between cytotoxicity and NQO1 activity, BAD protein levels and apoptosis, but not always between cytotoxicity and intracellular reactive oxygen species levels. The overall markedly increased cytotoxicity of the aziridinylbenzoquinone compounds used in this study is accompanied by apoptosis, which occurs mostly through a cytochrome *c*-independent pathway.

Keywords: Antitumor quinones; NQO1; Redox cycling; Hydroxyl radicals; Apoptosis; Cytochrome *c* release; BAD protein

1. Introduction

Current cancer drug discovery seeks to define candidate compounds that interact with molecular targets ideally unique to tumor cells, forming the basis for differential activity or toxicity of the drugs. The cytotoxicity of antitumor quinones has been attributed to the generation of ROS after redox cycling and/or to the alkylation of cellular nucleophiles [1,2]. Numerous attempts have been made to understand the contribution of these two different mechanisms influenced by the chemical structure of the compounds.

One potentially important target related to quinone action is the two-electron reductase NQO1, also known as DT-diaphorase [3]. NQO1 expression is highly increased in non-small cell lung cancer relative to the normal lung, and elevated levels of NQO1 mRNA and/or NQO1 activity have been found in a variety of tumor cell lines [4]. NQO1 can be induced in many tissues by quinone-based compounds [5] and by a wide variety of other compounds including dithiolethiones and isothiocyanates. The high level of NQO1 in tumor tissue, as compared to normal tissue [6,7], has made NQO1 a useful target for quinone-based bioreductive antitumor therapies [8]. An evaluation of individual patients and tumors for the presence of high levels of NQO1 activity may be necessary for optimal exploitation of this strategy, since there is extensive polymorphism in the population, due to homozygous point mutations that inactivate NQO1 [9,10].

☆Disclaimer: The content of this publication does not necessarily reflect the views or policies of the Department of Health and Human Services, nor does mention of trade names, commercial products, or organizations implying endorsement by the U.S. Government.

* Corresponding author. Tel.: +1-301-496-8720; fax: +1-301-402-0831.
E-mail address: sausville@nih.gov (E.A. Sausville).

Abbreviations: DCPIP, 2,6-dichlorophenol-indophenol; DMPO, 5,5-dimethyl-1-pyrroline-*N*-oxide; CM-H2DCFDA, 6-carboxy-2′,7′-dichlorodihydrofluorescein,di(acetoxymethyl ester); HE, hydroethidium; NQO1, NAD(P)H:quinone oxidoreductase; ROS, reactive oxygen species.

0006-2952/03/$ – see front matter © 2003 Elsevier Science Inc. All rights reserved.
doi:10.1016/S0006-2952(03)00013-3

NQO1 is a flavoprotein that catalyzes the two-electron reduction of quinones [11], quinoneimines [12], and quinone epoxides [13] to their hydroquinone derivatives, bypassing the semiquinone intermediates [11]. It can utilize NADH or NADPH as an electron source and is inhibited by Dicoumarol [14]. The reduced hydroquinones can further react in the cell to produce intermediate radical species. These radical metabolites have been shown to induce cellular damage by acting as alkylating agents and/or by inducing oxidative stress [15–17].

The physiological function of NQO1 remains unclear. It has been suggested that NQO1 activity offers protection against oxidative stress and carcinogens. Many instances have been reported where NQO1 appears to protect against quinone toxicity, where the hydroquinone product can be the substrate for cellular detoxification mechanisms [18–20]. NQO1 activity is also implicated in the reductive activation of antitumor quinones [21–23]. Examples of compounds that have been shown to be good substrates for NQO1 include: streptonigrin [24], the indoloquinone EO9 [25], the dinitrophenylaziridine CB1954 [26], mitomycin C [15,17,27], MeDZQ [28], and diaziquone [22,29]. The importance of NQO1 in the bioactivation of cytotoxic indolequinones, aziridinylbenzoquinones, and other compounds has already been established. The duality of NQO1 in the mode of action of bioreductive agents is typified by mitomycin C: NQO1 activates mitomycin C to an alkylating species under aerobic conditions but, under hypoxic conditions, NQO1 can act as a cellular protectant against the toxicity of mitomycin C [17,27].

The Developmental Therapeutics Program (DTP) of the National Cancer Institute has developed a bioinformatic approach [30] to correlate the patterns of *in vitro* growth inhibition by different anticancer agents of 60 different human tumor cell lines with the patterns of expression or activity of several molecular targets in these cells. In several instances, the expression of a molecular target can identify compounds whose action is mediated, in part, by that target. A strong correlation has been found previously between the *in vitro* sensitivities to mitomycin C or EO9 and the activity of the NQO1 reductase, but not the NADPH:cytochrome P450 or the NADH:cytochrome b_5 reductases [31]. More recently, a correlation has been found between the expression of NQO1 and the expression of the pro-apoptotic protein BAD in the 60 cell line panel [32]. We extend this analysis to define sets of quinones whose cytotoxicity correlates directly with the degree of NQO1 activity and BAD protein levels, or sets of quinones whose capacity for cytotoxicity correlates inversely, implying that NQO1 activity might be irrelevant to the action of the compound, or actually detoxify the compound.

We utilized two different human cell lines, the MCF-7 breast carcinoma cell line (high NQO1 activity and high BAD protein levels) and the HL-60 myeloid leukemia cell line (no NQO1 activity and low BAD protein levels). We adopted the hypothesis that "direct" quinones, whose toxicity is directly correlated with NQO1 activity in the 60 cell line panel would be activated by bioreduction and have a high capacity to induce apoptosis, whereas "inverse" quinones, with respect to cytotoxicity and NQO1 activity, would be less capable of bioreductive activation and have a correspondingly decreased capacity to induce apoptosis.

We did find a good correlation between the cytotoxic activity of the direct correlating quinones and their capacity for bioreduction by NQO1. However, we found two groups of directly correlating (with NQO1) quinones. In one, increased cytotoxicity correlated with increased BAD protein levels and induction of apoptotic cell death. However, the second and more cytotoxic compounds, the aziridinylbenzoquinones, did not necessarily generate higher levels of free radicals and induced apoptosis by a mechanism that apparently bypasses cytochrome *c* release. These results would suggest that non-mitochondrial mechanisms of evoking cell death could be initiated by cytotoxic quinones, in addition to mechanisms related to effects on mitochondria. Instead, the inverse correlating (with NQO1) quinones were, as expected, poor substrates for NQO1 and showed both decreased cytotoxicity and potential for inducing apoptosis.

2. Materials and methods

2.1. Materials

Compounds were obtained from the NCI Open Compound Repository, Drug Synthesis and Chemistry Branch, NCI. Stock solutions of drugs were made in DMSO and stored at −70°. Cytochrome *c* (beef heart), 3,3′-methylenebis[4-hydroxycoumarin] (Dicoumarol), DCPIP, NADH, NADPH, and EDTA were obtained from the Sigma Chemical Co. The spin trap DMPO was obtained from the Aldrich Chemical Co. CM-H_2DCFDA and HE were from Molecular Probes.

2.2. Cell culture and drug treatment

The HL-60 promyelocytic leukemia and MCF-7 breast carcinoma cell lines were obtained from the Biological Testing Branch, NCI. Cells were grown in RPMI-1640 medium (Life Technologies) with 10% fetal bovine serum, 5 mM L-glutamine, 100 ng/mL of penicillin, and 100 ng/mL of streptomycin at 37° in 5% CO_2. Before treatment, drugs were diluted in serum-free medium and used at a final concentration of <0.1% DMSO.

2.3. Preparation of S9 fractions

Exponentially growing cells were harvested, suspended in PBS, and washed three times. The cell pellets were resuspended in 1 mL of cold PBS and disrupted by homogenization. The homogenates were centrifuged at 1000 *g* for 10 min at 4°, and the resulting supernatants

were further centrifuged at 10,000 *g* for 30 min. The supernatants (S9 fractions) were collected and stored at −70°. The protein content of the S9 fractions was determined using the BCA Protein Assay (Pierce).

2.4. Cell viability and apoptosis assay

For the evaluation of cell viability in response to drug treatment, 3×10^6 cells were incubated with drug at concentrations known to induce total cell growth inhibition (TGI) by 24 hr. Cell viability was assayed by trypan blue exclusion at 0, 3, 6, and 24 hr. Triplicate samples were used for each treatment. Apoptosis was detected by flow-cytometry using the Annexin V-FITC apoptosis detection kit from Oncogene Research Products. Cells were incubated with drug for 0, 3, 6, and 24 hr at concentrations higher than those producing TGI. Following drug treatment, 5×10^5 cells were used for the conventional Annexin V binding protocol, according to the instructions of the manufacturer, and bivariate Annexin V/PI analysis was performed by flow cytometry.

2.5. Western blot analysis

Total proteins were isolated from $1–2 \times 10^7$ cells, lysed in 0.5 to 1 mL of lysis buffer [50 mM HEPES (pH 7.4); 150 mM KCl; 5 mM $MgCl_2$; 1 mM EGTA; 0.5% Nonidet P-40; 0.5 mM phenylmethylsulfonyl fluoride; 20 μM leupeptin; 20 μM aprotinin; 14 μM pepstatin A] by homogenization. Cell homogenates were centrifuged at 14,000 *g* for 30 min at 4°. Supernatants were collected and stored at −70°, until analyzed by gel electrophoresis. These lysates contained the cytosolic and light membrane fractions but not nuclei or mitochondria. Protein content in each lysate was determined by using the BCA Protein Assay (Pierce). Fifty micrograms of protein per lane was loaded on 12% Tris-glycine precast gels (Novex) and transferred in a submerged transfer unit (NOVEX Xcell II) to polyvinylidene fluoride (PVDF) membranes, in Tris glycine transfer buffer (NOVEX) containing 5% methanol. Membranes were then blocked in TBS containing 0.1% Tween-20 and 10% dry milk, at room temperature for 1 hr, and used for immunoblotting. The following primary antibodies were used: BAD, rabbit polyclonal (Transduction Laboratories, No. B31420); β-actin, mouse monoclonal (Sigma, No. A5441); and cytochrome *c*, mouse monoclonal (Pharmingen). Immunoblotting was performed using 2–5 μg of primary antibody and 1:2500 dilution of secondary antibody, in 10 mL of TBS containing 0.1% Tween 20 and 10% dry milk. Proteins were visualized using peroxidase-conjugated anti-mouse or anti-rabbit secondary antibodies and enhanced chemiluminescence (ECL) western blotting detection reagents (Amersham) as recommended by the manufacturer. The resulting immunoblot signals were quantified by densitometric scanning (Digital Imaging System from the Alpha Innotech Co.). The β-actin signal was used to normalize for the amount of protein loaded in each lane, and the results were expressed as fold-increase relative to untreated control (1×).

2.6. Cytochrome c quantitative ELISA

Cytochrome *c* was detected using the quantitative ELISA kit Quantikine (R&D Systems). Cells (2×10^3) were seeded in 96-well plates in triplicates and allowed to adhere overnight. Drugs were added, and the plates were incubated for 1, 3, 6, and 24 hr without removal of the drugs. Following drug treatment, cells were lysed in the plates, and the lysates were processed according to the instructions of the manufacturer. The amount of cytochrome *c* released in the cytosol (ng/mL) was calculated based on a standard curve generated using serial dilutions of human cytochrome *c*, as indicated in the kit. Two optical density readings were taken at 5 and 10 min following color development, as recommended by the manufacturer.

2.7. Assay for activity of the reductase enzymes in the MCF-7 and HL-60 S9 fractions

NAD(P)H oxidoreductase (NQO1) activity was measured spectrophotometrically (600 nm) using DCPIP as the electron acceptor and NADH as the reductant as described by others [11]. NQO1 activity was that activity inhibited by Dicoumarol (10 μM). NADPH:cytochrome P450 reductase activity was measured spectrophotometrically (550 nm) using cytochrome *c* as a substrate [33].

2.8. ESR measurements

ESR spectra were obtained at room temperature using a Varian E109 Century Series ESR spectrometer (Varian) equipped with a 100 kHz field modulation. A dual cavity (TE-104) was used with a strong pitch standard ($G = 2.0028$) in one section and the sample in a flat ESR cell in the other. Exponentially growing cells were harvested and suspended in 500 μL of PBS to a density of 10^7 cells/mL. The cell suspension was mixed rapidly with 1 mM compound and 100 mM DMPO. The mixture was quickly transferred to an ESR flat cell and placed in the ESR spectrometer for measurement. Control experiments were carried out as described above, in the absence of drug. The relative ability of the various quinones to produce hydroxyl radicals was evaluated by using the steady-state signal intensity of the DMPO–OH adduct.

2.9. Detection of peroxides and superoxides by flow cytometry

HL-60 and MCF-7 cells (1×10^6) were incubated with drug following the same conditions used for the apoptosis assay. CM-H_2DCFDA and HE, two sensitive fluorimetric

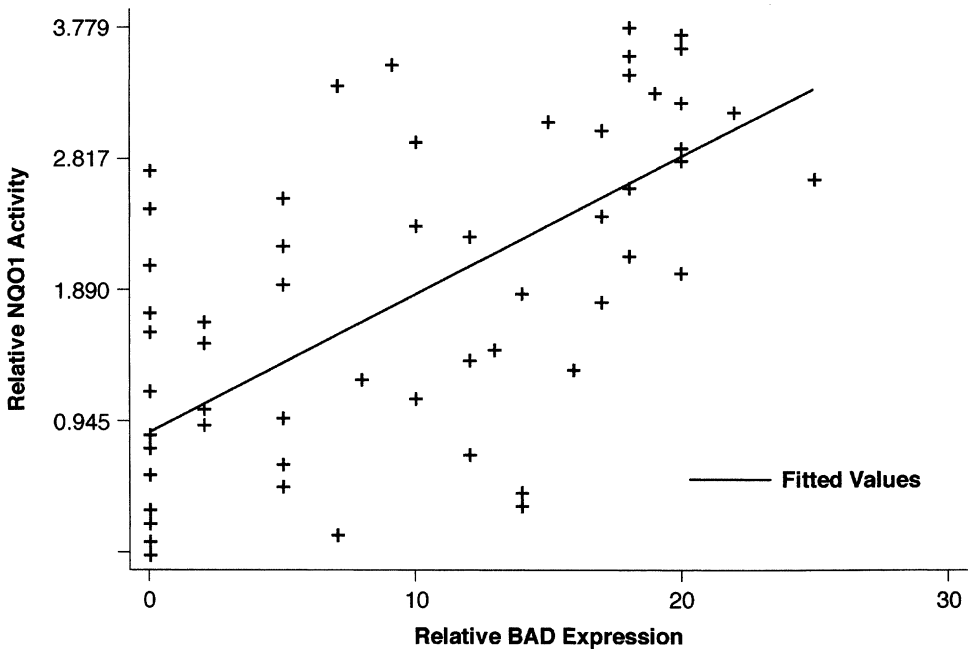

Fig. 1. Statistical correlation between BAD and NQO1 (DT-diaphorase). COMPARE algorithm-generated linear correlation between BAD protein levels [33] and NQO1 activity [32] in the 60 cell line panel of the NCI *in vitro* anticancer drug screen ($r = 0.58$; $P < 0.0001$; $N = 60$). The slope of the regression line is 1.445 ± 0.2.

probes of peroxides and superoxides respectively, were dissolved in DMSO and incubated with the cells for 30 min at 37°. H_2O_2 (20 mM) and antimycin A (50 μM) were used as positive controls for peroxides and superoxides, respectively. After incubation, the medium was removed and the cells were analyzed with a FACScan (Becton Dickinson).

3. Results

3.1. BAD and NQO1 expression

In an effort to define molecular correlates that would link the capacity of cells to undergo apoptosis with drug action, baseline levels of protein expression of the apoptosis modulators BCL2, BCL-X_L, BAK, BAD, BAG-1, and the IAP family in the NCI *in vitro* 60 cell line anticancer drug screen have been determined [32,34,35]. To further delineate associations of regulatory molecules important in apoptosis, we correlated the patterns of expression of these apoptotic proteins in the 60 cell lines with the expression of other molecular targets and compound anti-proliferative activities. As a result of this approach, a significant positive correlation ($r = 0.58$; $P < 0.0001$; $N = 60$) was found between BAD protein levels and NQO1 activity [32] (Fig. 1). Dephosphorylated BAD has been shown to relocate to the mitochondria where it binds to and antagonizes the cell survival promoting activity of BCL-2 and BCL-X_L [36,37]. The correlation between BAD and NQO1 therefore leads to the hypothesis that quinones activated by NQO1 are likely to activate a mitochondrial apoptotic program involving cytochrome *c* release.

3.2. Quinone compounds and cell lines

The cytotoxicity of several agents, mostly quinone-based compounds, correlated with the expression of both BAD and NQO1. Using the COMPARE algorithm (http://dtp.nci.nih.gov), two groups of compounds were selected, based on these correlations (Fig. 2). The direct correlating group A and B quinones (Fig. 2A) showed more potent cytotoxic activity in cell lines having high levels of BAD protein and NQO1 activity. The inverse correlating group C quinones (Fig. 2B) showed higher activity in cell lines with low BAD and low NQO1 levels. Group A compounds are aziridinylbenzoquinones, which are active antitumor agents containing both quinone and aziridine moieties. The A1 indoloquinone anticancer agent EO9 (NSC No. 382459) has been shown to be good substrate for NQO1, which plays an important role in the DNA cross-linking and sequence selectivity of this compound [38]. The strategy underlying the selectivity of these prodrugs is that a two-electron reduction of the quinone moiety markedly increases the electrophilicity of attached functional groups, thereby converting the prodrugs into DNA-alkylating species. The aziridine and hydroxyl groups have been implicated in activation to alkylating species after reduction, in addition to the generation of oxygen radical species. Group B compounds are directly correlated with NQO1 and BAD expression but do not have the aziridine moiety. Group C compounds, the 1,2-naphthoquinone and anthraquinone derivatives, are inversely correlated in their cytotoxicity with NQO1 and BAD expression. The non-quinone nitroaromatic compound B5c (NSC No. 673789) and the *p*-dihydrodiol C4c (NSC No. 306951) were used as "negative" controls in

Table 1
Basal levels of reductase activity, BAD protein, and p53 status in MCF-7 and HL-60 cells

Cell line	NQO1[a]	P450R[b]	BAD[c]	p53[d]
HL-60	7	22	0	–/–
MCF-7	242	16	14	w/w

[a] NQO1 activity levels in the cytosol (S9 supernatant) of HL-60 and MCF-7 cells, measured in nmol DCPIP reduced/min/mg protein [11], as described. Values are means of duplicate determinations.
[b] Cytochrome P450 reducatase activity of S9 pellets measured in nmol cytochrome *c* reduced/min/mg protein [33]. Values are means of duplicate determinations.
[c] Determined by relative expression in immunoblots [32].
[d] Determined by complete bidirectional p53 cDNA sequencing [39]. Key: –/– = null; w/w = wild-type.

these experiments, as it was expected that they would not be good substrates for redox-cycling and radical production.

Characteristics of the cells to be examined in detail here are shown in Table 1. MCF-7 breast carcinoma and HL-60 myeloid leukemia cell lines had different baseline levels of NQO1 and cytochrome P450. In the MCF-7 cells, the cytochrome *c* reductase activity was approximately 15 times less than the two-electron reduction activity of NQO1, whereas in the HL-60 cells the cytochrome *c* reductase activity was three times higher. The MCF-7 cells had relatively high baseline levels of the pro-apoptotic protein BAD and a wild-type p53 status, while HL-60 cells did not express detectable baseline levels of BAD protein and had a mutated p53 status.

3.3. Effect of quinone compounds on MCF-7 and HL-60 cell growth

Asynchronous populations of cells were treated with drug for 3, 6, and 24 hr and subsequently evaluated for survival (Fig. 3). As predicted by the COMPARE algorithm, the cytotoxicity of the directly correlated compounds was higher in the MCF-7 cells as compared with

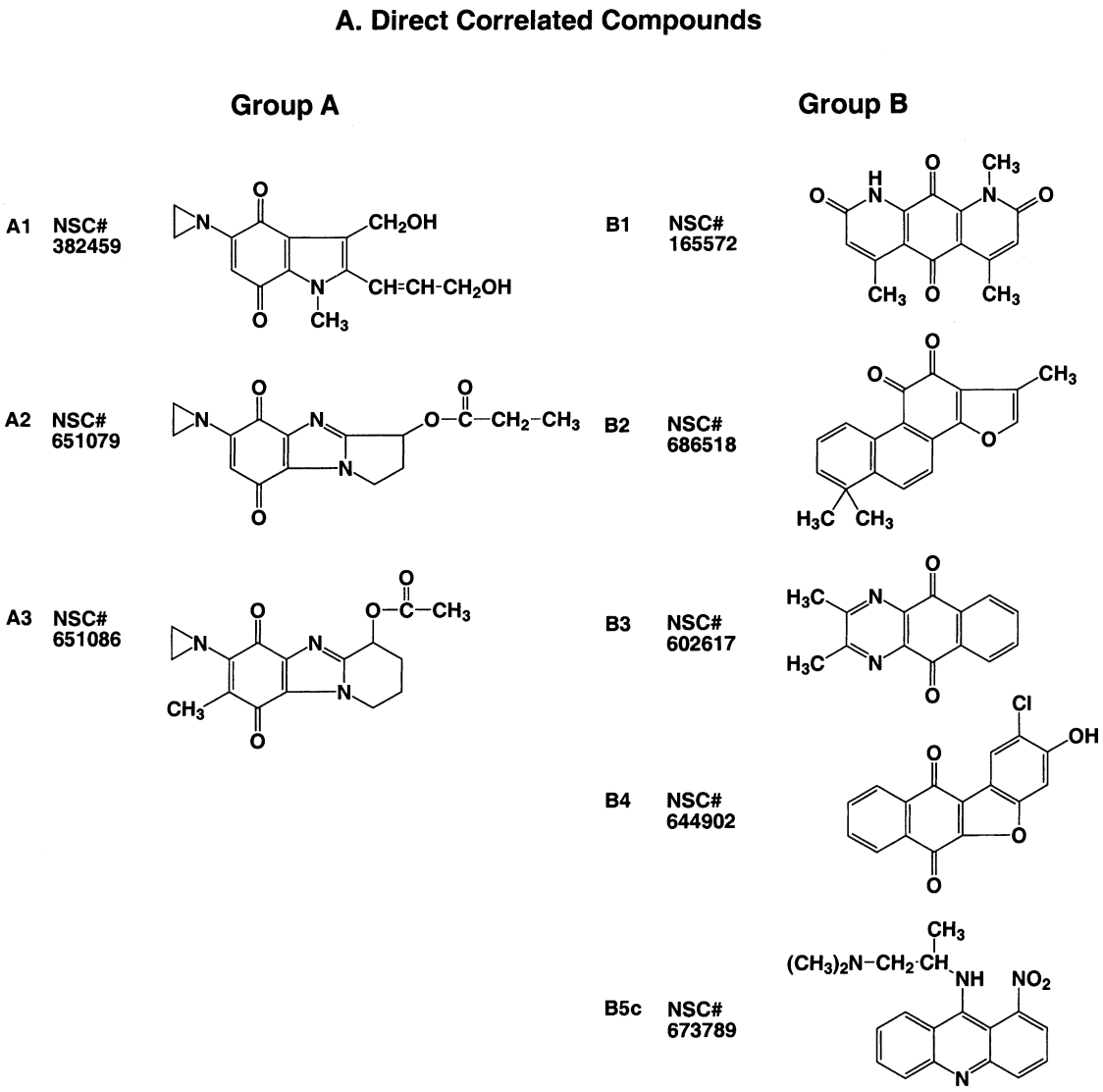

Fig. 2. Chemical structures of the quinone-based compounds used in this study.

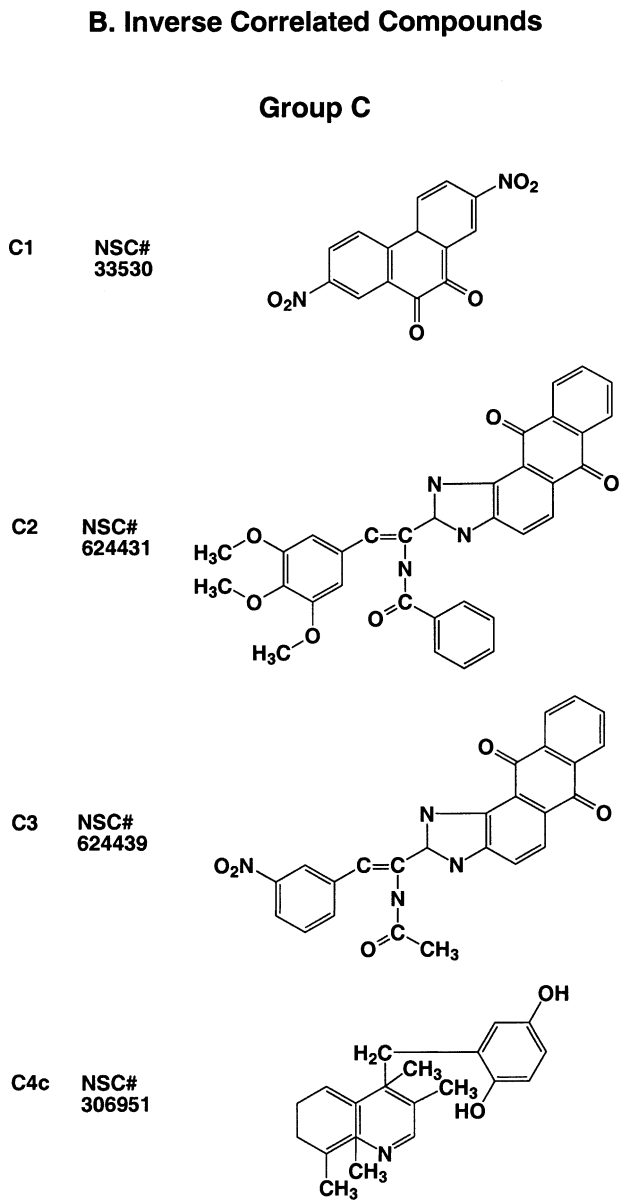

Fig. 2. (*Continued*).

the inverse correlated ones. Group A compounds inhibited the growth of MCF-7 cells at concentrations in the range of 0.01 to 0.1 μM. Group B compounds required 10- to 100-fold higher concentrations to induce similar levels of growth inhibition in these cells, with the exception of B1 (not plotted), which showed somewhat higher cytotoxic activity in both cell lines (0.1 to 1.0 μM). Group C compounds showed essentially no effect in MCF-7 cells at concentrations up to 100 μM. In contrast, in HL-60 cells, group C compounds induced complete inhibition of cell growth by 6 hr at concentrations <30 μM. This is in agreement with the statistical correlation which predicts good activity for group C compounds in cell lines with low BAD protein and NQO1 activity. In fact, in the HL-60 cells, an overlapping of the cytotoxic potency of A, B, and C compounds can be seen, in contrast to the markedly different toxicity of the A and C compounds in the MCF-7 cells.

3.4. Detection of drug-induced free radicals in whole cells by ESR

Bioreductive activation of quinone-containing anticancer agents involves reduction by one or two electrons, which is catalyzed by flavoenzymes using NADPH or NADH as electron donors [40,41]. In the case of a one-electron reduction by NADPH:cytochrome P450 reductase, the quinone is reduced to the semiquinone, which under aerobic conditions, is oxidized to the parent quinone, a process that results in the concomitant production of superoxide radical anions. The formation of the superoxide radical is the beginning of a cascade that generates hydrogen peroxide and hydroxyl radicals. In the case of a two-electron reduction by NQO1, the hydroquinone is produced. While some hydroquinones of antitumor agents are stable, others (e.g. diaziquone) can be oxidized by one electron at a time with the formation of the semiquinone and the parental compound and the generation of ROS [29,41,42]. In a whole cell system, which is the system used in this study, as opposed to a purified enzyme system, these characteristics are not well defined, and complex mixtures of one- and two-electron reductions can occur.

In the present study, we used the spin trap DMPO to detect the production of hydroxyl radicals, which is at the end of the cascade started by superoxides. Fig. 4A shows ESR spectra typical of the DMPO–OH adduct, which yielded a 1:2:2:1 quartet with typical ESR hyperfine couplings of $A_H^{\beta} = A_N = 14.9$ G. Because the compounds were dissolved in DMSO, this solvent provided an internal control used to eliminate the possibility of artifacts involved in the production of the observed DMPO–OH adduct, such as rearranging of the DMPO–superoxide adduct. The hydroxyl radicals react with DMSO producing a carbon-centered radical, which is then trapped by DMPO. This adduct yielded a 6-line triplet of doublets ESR spectrum with typical hyperfine coupling of $A_H = 23.1$ and $A_N = 16.5$ G, which can be clearly seen approximately 30 min after whole MCF-7 cells reduced the compound (Fig. 4C). The kinetic analysis of these data takes into account the rate of growth of a given line in the ESR spectrum. The rate of redox cycling for all compounds measured in the cell suspension at 4 and at 8 min is shown in Table 2.

Within the directly correlated compounds (groups A and B), there is variation in their bioreduction. Surprisingly, the semiquinones were detected very early in the reaction for some of the compounds. For instance, compound B1 (NSC No. 165572) showed a strong semiquinone 8 min after the onset of the reaction. At 12 min, the intensity of this semiquinone signal was 16-fold higher in MCF-7 cells than in HL-60 cells (data not shown). This fast formation of the semiquinone reflects both a fast redox cycling and a

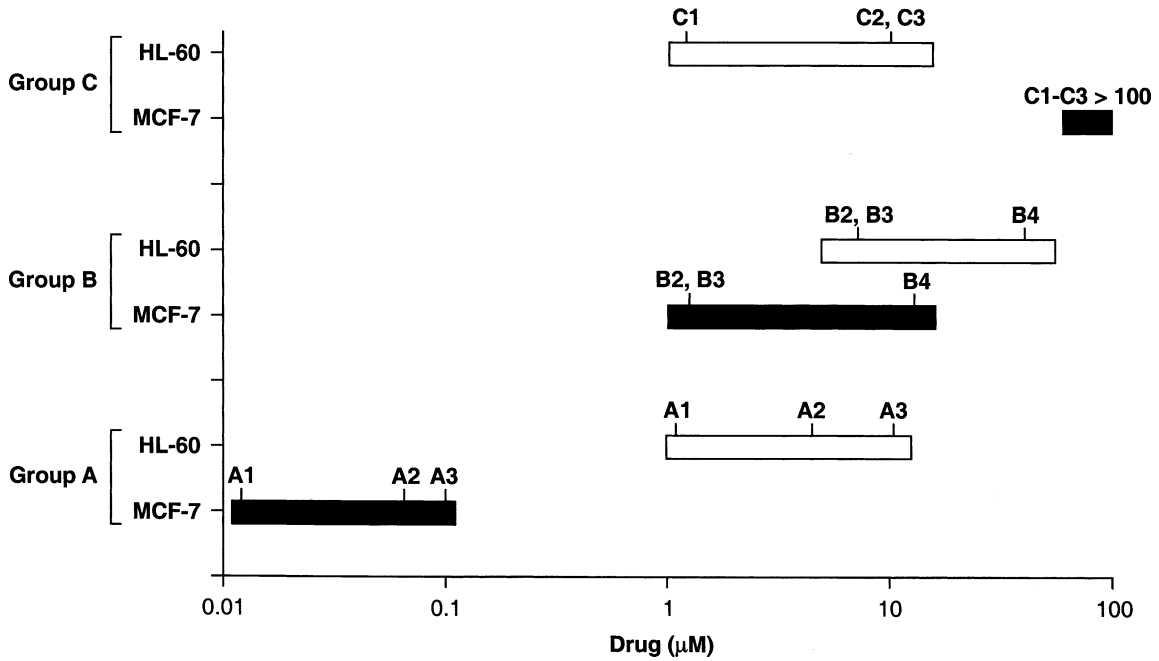

Fig. 3. Range of drug concentrations used to induce TGI (total growth inhibition) in the MCF-7 and HL-60 cells. Exponentially growing cells were exposed to drug concentrations known to inhibit cell growth by 24 hr (TGI). The cell viability was evaluated at 3, 6, and 24 hr by trypan blue exclusion. Values shown represent the range of drug concentrations for each group needed to induce cell growth arrest by 6 hr.

stable semiquinone (Fig. 4B). In general, the semiquinone is not detected until anaerobic conditions exist. In this case, the DMPO–OH signal disappeared quickly with the appearance of the semiquinone signal at 8 min. On the other hand, the compound may have the ability to form a stable semiquinone under partially aerobic conditions. It is interesting that this compound has almost as good cytotoxic activity as compounds from group A. Semiquinones of similar intensities were also detected for A3 (NSC No. 651086) and A1 (E09; NSC No. 382459) (not shown).

The data in Table 2 suggest that similar levels of free radicals are generated in the HL-60 and MCF-7 cells. However, group A compounds were better substrates for reduction by NQO1 in the MCF-7 cells, where they also were more cytotoxic. Group B compounds, on the other hand, redox cycled similarly well in both cell lines but were less cytotoxic in the HL-60 cells. Group C compounds did not redox cycle in MCF-7 cells but showed redox cycling in the HL-60 cells. This correlates with data showing no cytotoxicity in the MCF-7 cells at concentrations up to 100 μM when compared with higher levels of cytotoxicity in the HL-60 cells (Fig. 3). NSC compounds 673789 and 306951, thought to be poor substrates for redox cycling because of their chemical structure, were used as negative controls.

3.5. Determination of the intracellular redox state by flow cytometry

Fig. 5 shows an independent approach to documenting the generation of free radicals. We detected intracellular ROS as a function of drug concentration and time of exposure by using the fluorescent dye 2′7′-dichlorodihydrofluorescein diacetate (CM-H_2DCFDA) for the detection of peroxides and HE for the detection of superoxides. The nonenzymatic decomposition of H_2O_2 with the generation of hydroxyl radicals was used as a positive control for the detection of peroxides, and antimycin A, which generates superoxides efficiently in both cell lines, was used as a positive control for the detection of superoxides. Hydroquinone and thiotepa (an alkylating agent) were also used as controls in the two cell lines (Fig. 5D). The

Table 2
Comparison of hydroxyl radical formation mediated by quinone-based agents in whole MCF-7 and HL-60 cells by ESR at 4 and 8 min

Group No.	NSC No.	DMPO–OH (arbitrary units)			
		MCF-7 cells		HL-60 cells	
		4 min	8 min	4 min	8 min
A1	382459	19	22	17	9
A2	651079	27	26	22	28
A3	651086	27	26	17	16
B1	165572	20	Semiquinone	6	Semiquinone
B2	686518	16	16	24	28
B3	602617	30	33	39	42
B4	644902	16	22	13	22
B5 control	673789	0	5	0	0
C1	33530	0	0	0	8
C2	624431	0	0	7	10
C3	624439	0	0	11	11
C4 control	306951	0	0	8	9

Data are the signal intensities observed for the DMPO–OH adduct determined by measuring the peak to peak (P-P) height of the second low field line of the DMPO–OH adduct spectrum at 4 and 8 min after the onset of the reaction. Values are means of duplicate determinations.

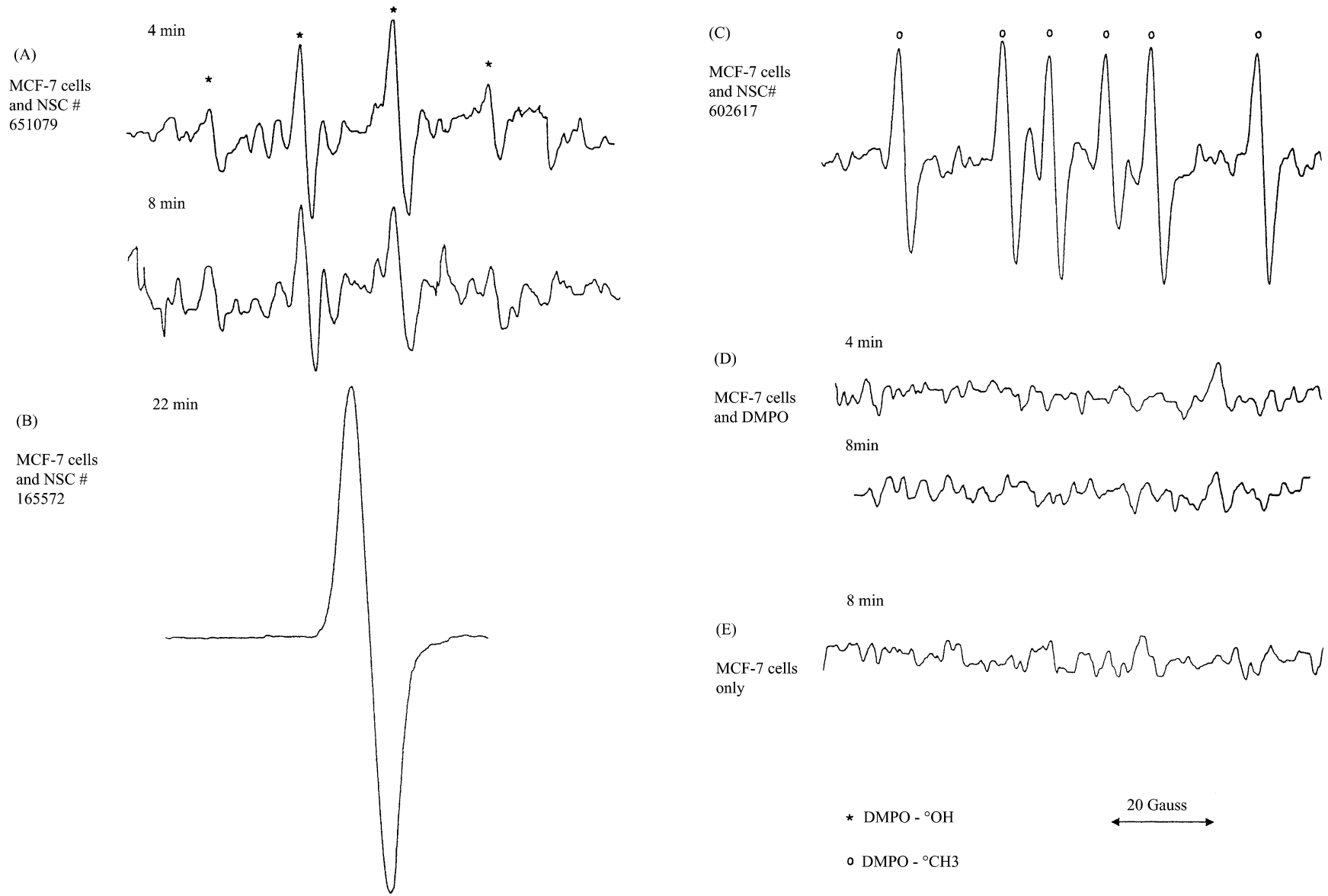

Fig. 4. ESR spectra of DMPO–OH adducts in whole MCF-7 and HL-60 cells. ESR spectra were obtained as described in Section 2 for a period of up to 30 min. Cells (10^7/mL) were rapidly mixed with 1 mM compound and 100 mM DMPO. The relative ability of the various quinones to produce hydroxyl radicals was evaluated by measuring the signal intensity of the DMPO–OH adduct. ESR spectra of MCF-7 cells in the presence of the direct correlating compound NSC No. 651079 at 4 and 8 min (A). The spectrum of the compound NSC No. 165572 at 22 min was taken at the same settings except the receiver gain was 1.25×10^4 (B). ESR spectrum of the DMPO–CH_3 adduct generated by DMSO used as an internal control to eliminate the possibility of artifacts involved in the production of the observed DMPO–OH adduct. This spectrum can be seen clearly after 30 min when whole MCF-7 cells reduced NSC No. 602617 (C). ESR spectra of MCF-7 cells and DMPO alone (D). ESR spectrum of MCF-7 cells in the absence of drug (E). ESR spectra are representative of one of two determinations.

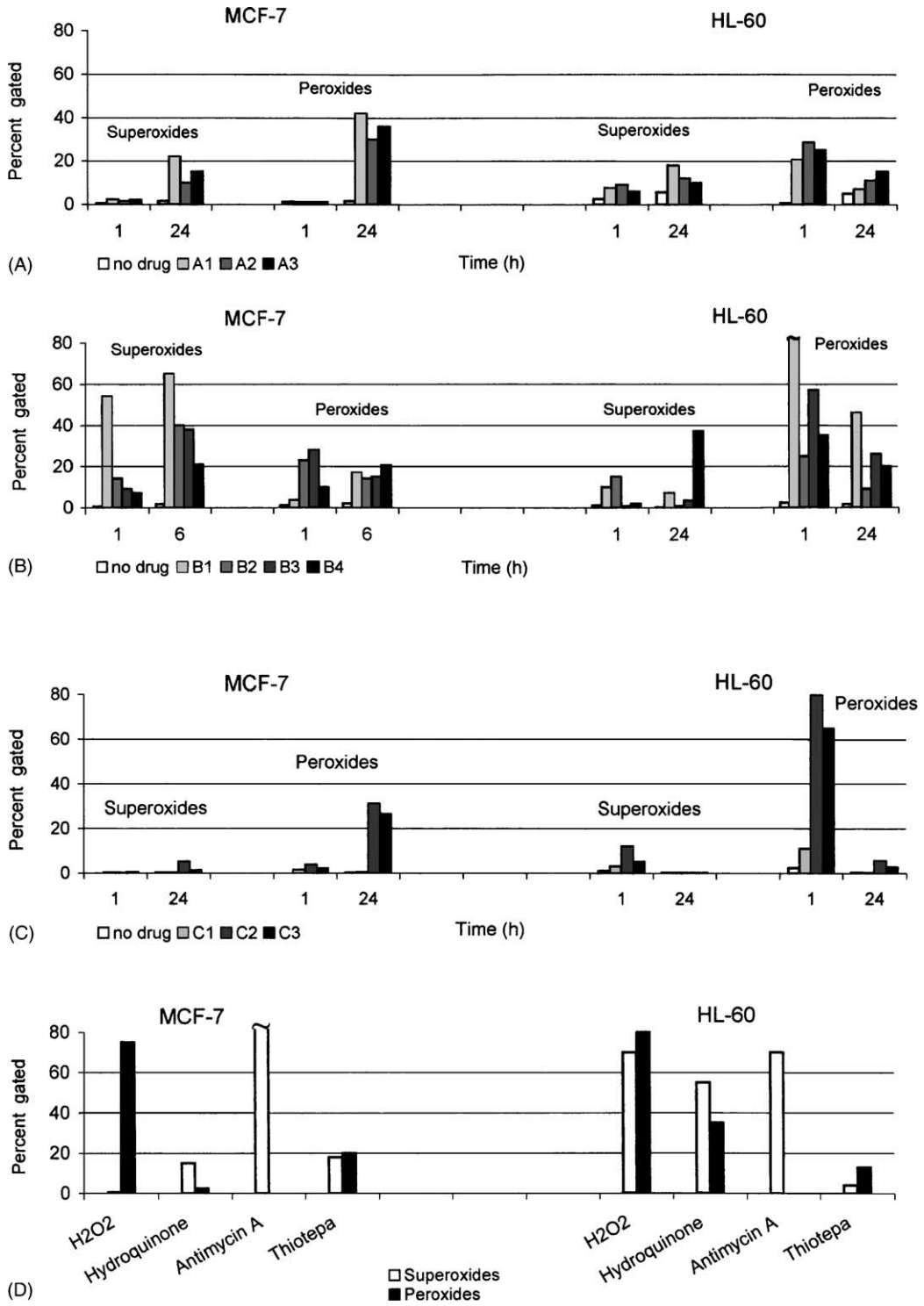

Fig. 5. ROS detection as CM-H_2DCFDA and HE oxidation in MCF-7 and HL-60 cells by flow cytometry. Cells were treated with drug for 1, 3, 6, 12, and 24 hr at the concentrations indicated below, followed by a 30-min treatment with CM-H_2DCFDA and HE. Data represent a bivariate flow cytometric analysis and are expressed as the percentage of cells showing a positive signal. Group A compounds: MCF-7 cells: A1: 0.2 μM; A2: 0.2 μM; A3: 0.2 μM. HL-60 cells: A1: 1 μM; A2: 1 μM; A3: 1 μM (A). Group B compounds: MCF-7 cells: B1: 0.5 μM; B2: 1 μM; B3: 5 μM; B4: 10 μM. HL-60 cells: B1: 1 μM; B2: 40 μM; B3: 40 μM; B4: 40 μM (B). Group C compounds: MCF-7 cells: C1: 100 μM; C2: 100 μM; C3: 100 μM. HL-60 cells: C1: 40 μM; C2: 40 μM; C3: 40 μM (C). MCF-7 cells: H_2O_2: 20 mM for 2 min; hydroquinone: 50 μM for 1 hr; antimycin A: 50 μM for 1 hr; thiotepa: 200 μM for 24 hr. HL-60 cells: H_2O_2: 20 mM for 2 min; hydroquinone: 25 μM for 3 hr; antimycin A: 50 μM for 3 hr; thiotepa: 200 μM for 24 hr (D). Values are means from three separate experiments.

kinetics of H_2DCF oxidation to fluorescent DCF and the oxidation of HE to ethidium were increased significantly in drug-treated cells as compared with untreated controls. Although the continuous exposure to toxic compounds should contribute substantially to the cellular steady-state concentrations of these species (H_2O_2 and $O_2^{\bullet -}$), the precise contribution of each species is difficult to assess because of a certain level of overlapping between the two fluorochromes and the rapid dismutation of superoxides to generate hydroxyl radicals. Peroxides were detected in the MCF-7 cells by this method only after prolonged exposure to group A compounds (24 hr), while higher concentrations of group A compounds generated lower levels of ROS in the HL-60 cells upon short treatment (1 hr) (Fig. 5A). In general, the higher cytotoxicity of the aziridinylbenzoquinones was not accompanied by higher levels of ROS. Group B compounds redox-cycled similarly well in both cell lines (Fig. 5B), although higher concentrations were required in the HL-60 cells, with the exception of B1. At 24 hr, redox-cycling of group B compounds was no longer detectable in the MCF-7 cells while it was still occurring in the HL-60 cells. B1, which generates semiquinones by ESR, showed very high levels of superoxides as expected in the MCF-7 cells, while the dismutation of its superoxide to H_2O_2 was very rapid in the HL-60 cells. Prolonged treatment of MCF-7 cells with C2 and C3 generated low levels of peroxides in the MCF-7 cells. On the contrary, these compounds generated high

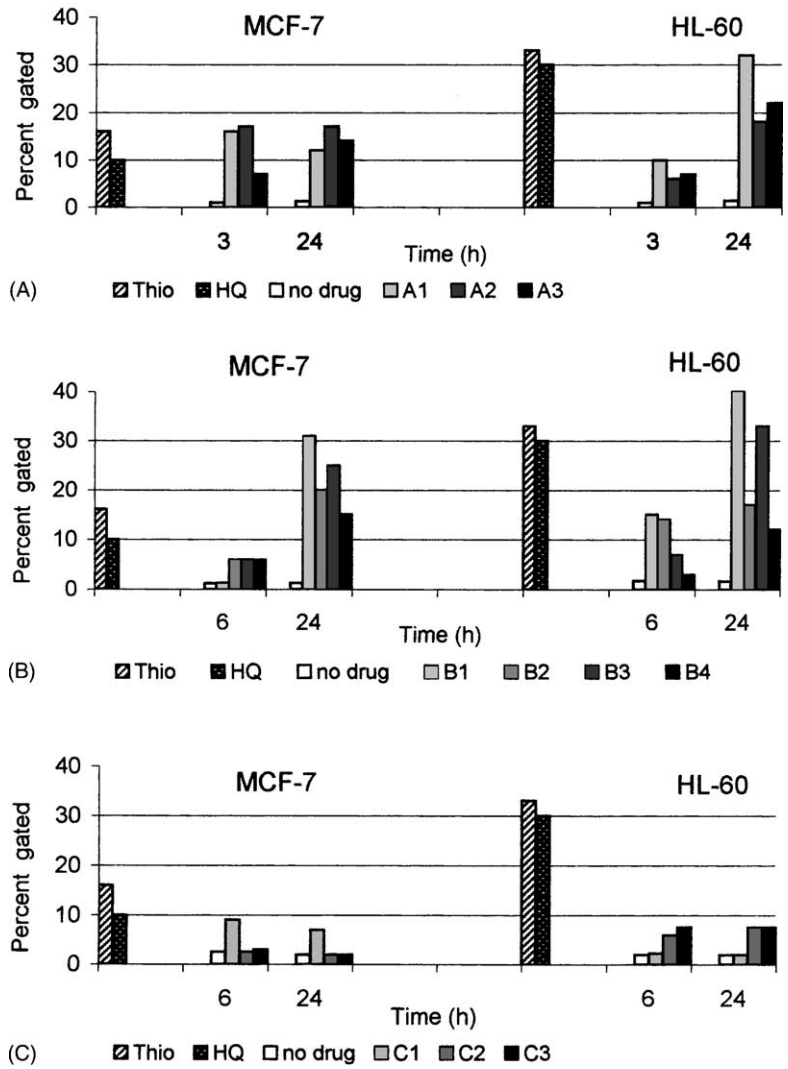

Fig. 6. Apoptosis detection in MCF-7 and HL-60 cells treated with quinone-based compounds. Apoptosis was measured by double staining with Annexin V and PI. Cells were treated with drug for 3, 6, and 24 hr at the concentrations indicated below and stained with Annexin V/PI according to the instructions of the manufacturer. Data represent the percentages of Annexin V positive and PI negative cells. Inducers of apoptosis used as positive controls in these experiments were thiotepa and hydroquinone. Group A compounds: MCF-7 cells: A1: 0.2 μM; A2: 0.2 μM; A3: 0.2 μM. HL-60 cells: A1: 1 μM; A2: 1 μM; A3: 1 μM (A). Group B compounds: MCF-7 cells: B1: 0.5 μM; B2: 1 μM; B3: 5 μM; B4: 10 μM. HL-60 cells: B1: 1 μM; B2: 40 μM; B3: 40 μM; B4: 40 μM (B). Group C compounds: MCF-7 cells: C1: 100 μM; C2: 100 μM; C3: 100 μM. HL-60 cells: C1: 40 μM; C2: 40 μM; C3: 40 μM (C). Thiotepa: 200 μM for 24 hr; hydroquinone: 50 μM for 3 hr. Values are the means from three separate experiments.

levels of peroxides in the HL-60 cells after only 1 hr of treatment (Fig. 5C).

3.6. Apoptosis induction by benzoquinone compounds in the MCF-7 and HL-60 cells

Apoptosis was measured by assessing the externalization of phosphatidylserine (PS), an early event during apoptosis, by double staining with Annexin V and PI. The percentages of Annexin V positive and PI negative cells are shown in Fig. 6. As expected, low concentrations of group A compounds (nanomolar range) induced apoptosis in the MCF-7 cells but not in the HL-60 cells. Low levels of apotosis were detected as early as 3 hr in the MCF-7 cells (Fig. 6A) as opposed to the ROS detection which was evident after 24 hr of treatment (Fig. 5A). At higher concentrations (micromolar), group A compounds induced apoptosis in the HL-60 cells effectively (Fig. 6A), following the rapid generation of ROS (Fig. 5A). Group B compounds required higher concentrations in HL-60 cells to induce similar levels of apoptosis, which became evident after the detection of ROS (Fig. 6B). B1 and B3 showed both the highest levels of peroxides and the highest levels of apoptosis in these cells. Interestingly, C1 induced some apoptosis in the MCF-7 cells at high concentrations (Fig. 6C), in the absence of ROS generation (Fig. 5C). C2 and C3 were probably metabolized and detoxified with ROS generation (Fig. 5C), in the absence of cytotoxicity or apoptosis (Fig. 6C). Furthermore, C2 and C3, which generated ROS and were cytotoxic in the HL-60 cells (Fig. 5C), did not induce significant levels of apoptosis at equimolar concentrations (Fig. 6C), which suggests death by other mechanisms.

3.7. BAD protein expression and cytochrome c release

We have shown previously [43] that MCF-7 and HL-60 cells treated with the microtubule disruptor paclitaxel and the alkylating agent thiotepa show an early up-regulation of BAD, in response to cellular stress, which precedes the release of cytochrome *c* from mitochondria and apoptosis. As the cytotoxicity of quinone compounds studied here was associated with the generation of ROS and oxidative damage, we asked whether a similar modulation of BAD levels in conjunction with cytochome *c* release correlated with the cytotoxic activity of these quinones. Given the transient nature of BAD up-regulation [43], we measured the increase in BAD protein levels after 3, 6, and 24 hr of continuous treatment with drug, as compared with the untreated control at 3, 6, and 24 hr. The increase in BAD protein occurred as early as 3 hr and at varying degrees, depending on the compound used. Fig. 7 shows the average levels of BAD protein in the MCF-7 and HL-60 cells after 6 hr of treatment with compounds from each of the three groups, and the average levels of cytochrome *c* being released into the cytosol of the same cells, respectively. Group A and B compounds induced an ~2-fold increase in

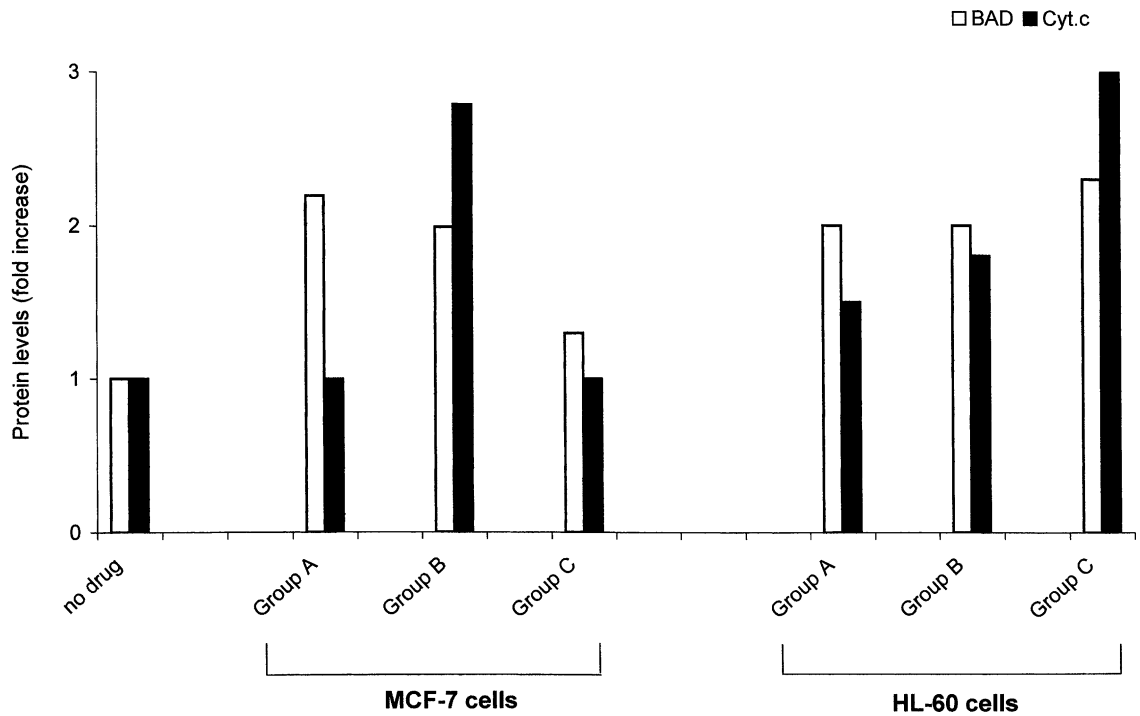

Fig. 7. Western blot analysis of BAD and cytochrome *c* in MCF-7 and HL-60 cells following treatment with quinone compounds. Cells were treated with drug as indicated in Fig. 6. Lysates were prepared and assessed by immunoblotting as described in Section 2. The bars represent the fold-increase in protein levels in the presence of drug as compared with the baseline levels in the absence of drug. Represented is the mean of the measurements in each group of drugs at 6 hr in the MCF-7 and HL-60 cells. Results are representative of one of two separate experiments.

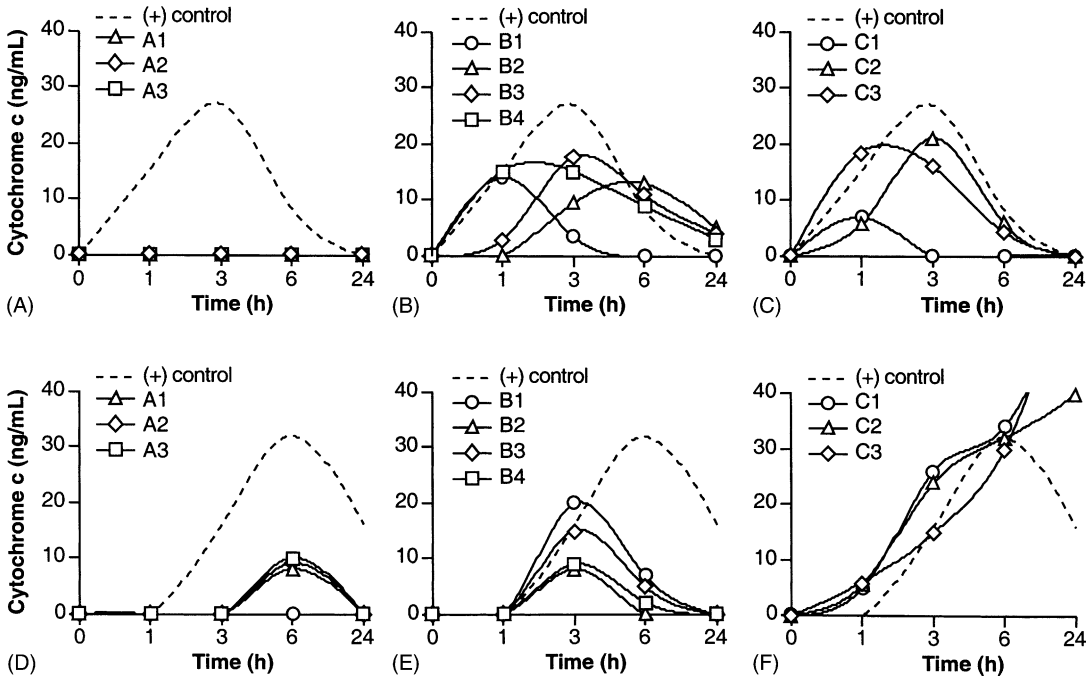

Fig. 8. Quantitative ELISA for the detection of cytochrome *c* release in the cytosol of MCF-7 and HL-60 cells following treatment with quinone compounds. Lysates were prepared at 1, 3, 6, and 24 hr and processed according to the instructions of the manufacturer (ELISA kit Quantikine; R&D Systems). The cytochrome *c* levels in the cytosol (ng/mL) were calculated as indicated in the kit. Positive controls were MCF-7 and HL-60 cells treated with 100 μM thiotepa for 3 hr. MCF-7 cells were treated with group A and B compounds as described in Fig. 6 (panels A and B); MCF-7 cells were treated with group C compounds at high concentrations: C1: 100 μM; C2: 200 μM; C3: 200 μM (panel C); HL-60 cells were treated with group A, B and C compounds as described in Fig. 6 (panels D, E, and F). Results are the means of two independent experiments involving triplicate determinations.

BAD protein levels as compared with baseline. Interestingly, group A compounds, which have the highest cytotoxicity and apoptotic rate in the MCF-7 cells, did not induce the release of cytochrome *c* in these cells, whereas group B compounds induced a >2-fold increase. Group C compounds, as expected, showed little or no release of cytochrome *c* in the MCF-7 cells. Clearly, there was an increase in cytochrome *c* release following treatment of the HL-60 cells with the group C compounds but, given the low level of apoptosis, it could have been the result of mostly necrotic death.

To confirm that the immunoblot method was accurate in this respect, an independent assay for the detection of cytochrome *c* by immunocapture and enzymatic assay was conducted over the 24-hr period following exposure to drugs (Fig. 8). Fig. 8A demonstrates that in the case of the MCF-7 cells, the group A compounds did not induce the release of detectable levels of cytochrome *c*, despite potent growth inhibition and evidence of apoptosis (Figs. 3 and 6, respectively). In contrast, all group B compounds showed evidence of efficient cytochrome *c* release by 6 hr after exposure to drug (Fig. 8B). The lack of detectable cytochrome *c* release by the group A aziridinylquinones would suggest the activation of a distinct apoptotic pathway by A compounds as compared to the B group. Group C compounds did not induce cytochrome *c* release in the MCF-7 cells at concentrations $\leq$100 μM, but they did when higher concentrations were being used (Fig. 8C). As expected from Fig. 6, in the HL-60 cells, higher concentrations of group A and B compounds all showed some capacity to release cytochrome *c* in these cells. Interestingly, in the HL-60 cells, high concentrations of group A compounds induced only low levels of cytochrome *c* release (Fig. 8D) and group B lower than in the MCF-7 cells (Fig. 8E). This correlates well with the lower cytotoxicity of these compounds in the HL-60 cells, despite obvious evidence of hydroxyl radicals in these cells. Finally, the cytotoxicity of group C compounds resulted in the release of cytochrome *c* in the HL-60 cells.

4. Discussion

The experiments presented here demonstrate that the computational algorithm COMPARE can define quinones that correlate in their cytotoxicity directly or inversely with NQO1 activity and with the baseline levels of BAD protein expression in the NCI *in vitro* 60 cell line anticancer drug screen. Among the directly correlating quinones, group A compounds have an aziridine functional group whereas group B compounds do not. The increased cytotoxicity of the directly correlating group A and B compounds was consistent with the effect of high levels of NQO1. Group B compounds showed efficient production of ROS irrespective of high or low NQO1 expression and high levels of free radicals did not always correlate with higher cytotoxicity.

Group C compounds comprise inversely correlating quinones whose cytotoxicity is actually lower in the setting of high NQO1 expression. As predicted by the COMPARE algorithm, group C compounds did not redox cycle well when compared with compounds that directly correlate NQO1 activity to high cytotoxicity. Both group A and B compounds, but not group C, efficiently elevated BAD protein levels in MCF-7 cells. Surprisingly, group A compounds did not release mitochondrial cytochrome *c* even as they gave evidence of apoptosis in either a high or low NQO1-expressing background. Therefore, our experiments would indicate that BAD induction does not always correlate with evidence of cytochrome *c* release.

Two types of benzoquinones were used in this study: the aziridinylbenzoquinones and those which do not have the aziridine molecule(s). Generally, the aziridinylquinones inhibit tumor growth by cross-linking guanine molecules of the double-stranded DNA and by generating radical intermediates, mostly from the benzoquinone moiety. There is a general consensus that both redox cycling and alkylation can induce oxidative stress and cell killing, but the molecular mechanisms involved in cell death are not fully understood. It has been shown that the bioreductive activation of some antitumor quinones by NQO1 can trigger apoptosis with higher incidence in cells with higher baseline levels of NQO1 [44]. However, it is not clear yet if apoptosis is a consequence of oxidative stress *per se*, drug-induced DNA damage, or activation of separate mechanisms in response to cell death signaling. Given the prominent capacity of aziridinyl ring-system containing compounds to interact with and cross-link DNA, one hypothesis to emerge from these data is that DNA-directed quinones may engage different mechanisms of apoptosis than compounds that do not efficiently cause DNA lesions. The higher activity of aziridinyl compounds would indicate the existence of such a cell death-inducing mechanism.

To evaluate the reactivity of these compounds as substrates for bioreductive activation, we looked at the levels of free radicals in a whole cell system under aerobic conditions. Here we provide direct ESR evidence for ROS formation from the metabolism of antitumor quinone compounds in MCF-7 and HL-60 cells and evidence for the generation of free radicals by the oxidation of the ROS-sensitive dyes CM-H_2DCFDA and HE. The identity of the toxic metabolic intermediates generated by these reactions is not the focus of this study, and the generation of free radicals is not used here as an endpoint of metabolic activation. Instead, the generation of free radicals as a result of redox-cycling is being correlated here to endpoints of metabolic activation such as cytotoxicity and apoptosis.

The redox cycling of group A and B compounds generates similar levels of hydroxyl radicals in MCF-7 cells. This would indicate that the greater cytotoxicity of the group A compounds is only in part the result of ROS production. The higher levels of radicals detected in response to group A compounds in the MCF-7 cells as compared with the HL-60 cells would suggest that the cytotoxicity of the aziridinyl compounds is potentiated by NQO1 activation. After increasing the concentrations of the group A compounds by more than 10-fold, cytotoxicity became also evident in the HL-60 cells, in agreement with the COMPARE algorithm, which predicts less potent activity in these cells.

The onset and therefore the detection of apoptosis induced by group A compounds in MCF-7 cells occurred earlier than the detection of ROS, in contradistinction to the HL-60 cells. This would be consistent with the idea that the cytotoxicity of the aziridinylbenzoquinones in the setting of high NQO1 activity in the MCF-7 cells is again only in part the result of ROS production. In contrast, group B compounds generated similar levels of ROS in the HL-60 and MCF-7 cells, and apoptosis induction by group B compounds became detectable after the onset of ROS generation in both cell lines, implying direct involvement of ROS in the apoptotic cell death. This was especially true for B1 and B3 compounds, which showed a direct correlation between hydroxyl radicals, apoptosis, and cytochrome *c* release. Since the active redox cycling and ROS generation do not appear to always correlate with cytotoxicity, the increased cytotoxicity of the aziridinylbenzoquinones in the MCF-7 cells in the absence of a proportional increase in ROS could imply the generation of deleterious hydroquinone intermediates. However, semiquinones have been detected for A1, A2, A3, and B1 compounds, and, in fact, the striking result was the appearance of semiquinone intermediates very early in the reaction.

Group C compounds do not generate hydroxyl radicals in MCF-7 cells, as determined by ESR. Oxidation of CM-H_2DCFDA and HE occurred only after prolonged exposure of MCF-7 cells to high concentrations of C1 and C2. Given the total absence of apoptosis or cell death at this time, the presence of ROS could possibly indicate the metabolism and detoxification of these drugs by MCF-7 cells.

Studies performed in recent years have demonstrated that there are two major pathways for inducing apoptosis: one mediated through activation of cell surface death receptors and another that involves mitochondrial damage and release of cytochrome *c* [45]. The translocation of cytochrome *c* from the intermembrane space of mitochondria to the cytoplasm is a crucial step in the transmission and amplification of many types of death signals through activation of caspases [45]. Activation of apoptotic pathways in the absence of cytochrome *c* release has also been reported [46,47]. Several studies indicated that mitochondrial dysfunction and cellular energy depletion play a major role in the mechanism of cell killing by quinones with differing structure and chemical reactivity [48].

Our results show that higher cytotoxicity does not necessarily correlate with damage to the mitochondria manifested as cytochrome *c* release. In fact, group A compounds, which showed the highest activity in MCF-7 cells, did not induce cytochrome *c* release as a mechanism of apoptosis induction. At higher concentrations, they induced

the release of only limited levels of cytochrome *c* into the cytoplasm of HL-60 cells. In contrast, group B compounds induced cytochrome *c* release in both cell lines. Group C compounds induced cytochrome *c* release in the HL-60 cells and only at higher concentrations (200 μM) in the MCF-7 cells. The lack of significant release of cytochrome *c* into the cytosol in response to the faster acting aziridinylquinones as compared to the other quinones might indicate the activation of separate signaling pathways leading to apoptosis in cell lines that can efficiently activate these compounds.

In conclusion, an evident correlation exists between the cytotoxicity of the compounds, the activity of NQO1, the increase in BAD protein, and the induction of apoptosis. The production of free radicals does not always correlate with cytotoxicity and apoptosis. BAD could act as an early response to stress, as part of the apoptotic signaling events. While the increase in BAD protein levels does not necessarily correlate with cytochrome *c* release, its relation to downstream effects on mitochondrial physiology remains to be mechanistically addressed. Future studies into the role of apoptotic regulators would be helpful in understanding the differential cytotoxicity of these compounds.

The results presented here underline the utility of computational analysis in selecting antitumor agents with similar mechanisms of action in relation to a particular molecular target. The COMPARE algorithm was capable of distinguishing between antitumor quinones, which were good or poor substrates for bioreductive activation. Furthermore, quinone-based compounds directly correlating with NQO1 activity showed high cytotoxicity in the context of high endogenous levels of the pro-apoptotic protein BAD, but among the direct correlating compounds there are clear differences in the type of apoptotic program being activated. Further elucidation of apoptotic mechanisms shared by the pro-apoptotic protein BAD and NQO1-activated drugs is currently underway.

Acknowledgments

This project was funded with Federal funds from the National Cancer Institute, National Institute of Health, under Contract N01-C0-12400.

References

[1] Miller M, Rodgers A, Cohen GM. Mechanisms of toxicity of naphthoquinones to isolated hepatocytes. Biochem Pharmacol 1986;35:1117–84.

[2] Toxopeus C, van Holsteijn I, Thuring JW, Blaauboer BJ, Noordhoek J. Cytotoxicity of menadione and related quinones in freshly isolated hepatocytes: effects on thiol homeostasis and energy charge. Arch Toxicol 1993;67:674–9.

[3] Robertson N, Stratford IJ, Houlbrook S, Carmichael J, Adams GE. The sensitivity of human tumor cells to quinone bioreductive drugs: what role for DT-diaphorase? Biochem Pharmacol 1992;44:409–12.

[4] Malkinson AM, Siegel D, Forrest GL, Gazdar AF, Oie HK, Chan DC, Bunn PA, Mabry M, Dykes DJ, Harrison Jr SD, Ross D. Elevated DT-diaphorase activity and messenger RNA content in human non-small cell lung carcinoma: relationship to the response of lung tumor xenografts to mitomycin C. Cancer Res 1992;52:4752–7.

[5] Beyer RE, Segura-Aguilar J, Lind C, Castro VM. DT-diaphorase activity in various cells in culture with emphasis on induction in ascites hepatoma cells. Chem Scripta 1987;27A:145–50.

[6] Cresteil T, Jaiswal AK. High levels of expression of the NAD(P)H:-quinone oxidoreductase (NQO_1) gene in tumor cells compared to normal cells of the same origin. Biochem Pharmacol 1991;42:1021–7.

[7] Jarrett CM, Bibby MC, Phillips RM. Bioreductive enzymology of malignant and normal human tissues. Proc Am Assoc Cancer Res 1998;39:429–36.

[8] Beall HD, Murphy AM, Siegel D, Hargreaves RHJ, Butler J, Ross D. Nicotinamide adenine dinucleotide (phosphate):quinone oxidoreductase (DT-diaphorase) as a target for bioreductive antitumor quinones: quinone cytotoxicity and selectivity in human lung and breast cancer cell lines. Mol Pharmacol 1995;48:499–504.

[9] Traver RD, Siegel D, Beall HD, Phillips RM, Gibson NW, Franklin WA, Ross D. Characterization of a polymorphism in NAD(P)H:quinone oxidoreductase (DT-diaphorase). Br J Cancer 1997;75:69–75.

[10] Kelsey KT, Ross D, Traver RD, Christiani DC, Zuo ZF, Spitz M, Wang M, Xu X, Lee BK, Schwartz BS, Wiencke JK. Ethnic variation in the prevalence of a common NAD(P)H:quinone oxidoreductase polymorphism and its implications for anticancer chemotherapy. Br J Cancer 1997;76:852–4.

[11] Ernster L. DT-diaphorase. Methods Enzymol 1967;10:309–17.

[12] Powis G, See KL, Santone KS, Melder DC, Hodnett EM. Quinoneimines as substrates for quinone reductase (NAD(P)H:(quinone-acceptor) oxidoreductase) and the effect of dicumarol on their cytotoxicity. Biochem Pharmacol 1987;36:2473–9.

[13] Brunmark A, Cadenas E, Lind C, Segura-Aguilar J, Ernster L. DT-diaphorase-catalyzed two-electron reduction of quinone epoxides. Free Radic Biol Med 1987;3:181–8.

[14] Edwards YH, Potter J, Hopkinson DA. Human FAD-dependent NAD(P)H diaphorase. Biochem J 1980;187:429–36.

[15] Siegel D, Gibson NW, Preusch PC, Ross D. Metabolism of mitomycin C by DT-diaphorase: role in mitomycin C-induced DNA damage and cytotoxicity in human colon carcinoma cells. Cancer Res 1990;50:7483–9.

[16] Gibson NW, Hartley JA, Butler J, Siegel D, Ross D. Relationship between DT-diaphorase-mediated metabolism of a series of aziridinylbenzoquinones and DNA damage and cytotoxicity. Mol Pharmacol 1992;42:531–6.

[17] Ross D, Siegel D, Beall HD, Prakash AS, Mulcahy RT, Gibson NW. DT-diaphorase in activation and detoxification of quinones. Bioreductive activation of mitomycin C. Cancer Metastasis Rev 1993;12:83–101.

[18] Lind C, Hochstein P, Ernster L. DT-diaphorase as a quinone reductase: a cellular control device against semiquinone and superoxide radical formation. Arch Biochem Biophys 1982;216:178–85.

[19] Thor H, Smith MT, Hartzell P, Bellomo G, Jewell SA, Orrenius S. The metabolism of menadione (2-methyl-1,4-naphthoquinone) by isolated rat hepatocytes. J Biol Chem 1982;257:12419–25.

[20] Atallah AS, Landolph JR, Ernster L, Hochstein P. DT-diaphorase activity and the cytotoxicity of quinones in CH3/10T1/2 mouse embryo cells. Biochem Pharmacol 1988;37:2451–9.

[21] Ross D, Siegel D, Gibson NW, Pacheco D, Thomas DJ, Reasor M, Wierda D. Activation and deactivation of quinones catalyzed by DT-diaphorase. Evidence for bioreductive activation of diaziquone (AZQ) in human tumor cells and detoxification of benzene metabolites in bone marrow stroma. Free Radic Res Commun 1990;8:373–81.

[22] Siegel D, Gibson NW, Preusch PC, Ross D. Metabolism of diaziquone by NAD(P)H:(quinone-acceptor) oxidoreductase (DT-diaphorase):

role in diaziquone-induced DNA damage and cytotoxicity in human colon carcinoma cells. Cancer Res 1990;50:7293–300.
[23] Keyes SR, Rockwell S, Sartorelli AC. Enhancement of mitomycin C cytotoxicity to hypoxic tumor cells by dicoumarol *in vivo* and *in vitro*. Cancer Res 1985;45:213–6.
[24] Beall HD, Liu Y, Siegel D, Bolton EM, Gibson NW, Ross D. Role of NAD(P)H:quinone oxidoreductase (DT-diaphorase) in cytotoxicity and induction of DNA damage by streptonigrin. Biochem Pharmacol 1996;51:645–52.
[25] Walton MI, Bibby MC, Double JA, Plumb JA, Workman P. DT-diaphorase activity correlates with sensitivity to the indoloquinone E09 in mouse and human colon carcinomas. Eur J Cancer 1992;28A:1597–600.
[26] Knox RJ, Boland MP, Friedlos F, Coles B, Southan C, Roberts JJ. The nitroreductase enzyme in Walker cells that activates 5-(aziridin-1-yl)-2,4-dinitrobenzamide (CB1954) to 5-(aziridin-1-yl)-4-hydroxylamino-2-nitrobenzamide is a form of NAD(P)H dehydrogenase (quinone) (EC 1.6.99.2). Biochem Pharmacol 1988;37:4671–7.
[27] Siegel D, Hartman C, Beall H, Kasai M, Arai H, Gibson NW, Ross D. Bioreductive activation of mitomycin C by DT-diaphorase. Biochemistry 1992;31:7879–85.
[28] Lee CS, Hartley JA, Berardini MD, Butler J, Siegel D, Ross D, Gibson NW. Alteration in DNA cross-linking and sequence selectivity of a series of aziridinylbenzoquinones after enzymatic reduction by DT-diaphorase. Biochemistry 1992;31:3019–25.
[29] Fisher GR, Gutierrez PL. The reductive metabolism of diaziquone (AZQ) in the S9 fraction of MCF-7 cells: free radical formation and NAD(P)H:quinone-acceptor oxidoreductase (DT-diaphorase) activity. Free Radic Biol Med 1991;10:359–70.
[30] Paull KD, Shoemaker RH, Hodes L, Monks A, Scudiero DA, Rubinstein L, Plowman J, Boyd MR. Display and analysis of patterns of differential activity of drugs against human tumor cell lines: development of mean graph and COMPARE algorithm. J Natl Cancer Inst 1989;81:1088–92.
[31] Fitzsimmons SA, Workman P, Grever M, Paull K, Camalier R, Lewis AD. Reductase enzyme expression across the National Cancer Institute tumor cell line panel: correlation with sensitivity to mitomycin C and EO9. J Natl Cancer Inst 1996;88:259–69.
[32] Kitada S, Krajewska M, Zhang X, Scudiero D, Zapata JM, Wang H-G, Shabaik A, Tudor G, Krajewski S, Myers TG, Johnson GS, Sausville EA, Reed JC. Expression and location of pro-apoptotic Bcl-2 family protein BAD in normal human tissues and tumor cell lines. Am J Pathol 1998;152:51–61.
[33] Strobel HW, Dignam JD. Purification and properties of NADPH-cytochrome P-450 reductase. Methods Enzymol 1978;52:89–96.
[34] Takayama S, Krajewski S, Krajewska M, Kitada S, Zapata JM, Kochel K, Knee D, Scudiero D, Tudor G, Miller GJ, Miyashita T, Yamada M, Reed JC. Expression and location of Hsp70/Hsc-binding anti-apoptotic protein BAG-1 and its variants in normal tissues and tumor cell lines. Cancer Res 1998;58:3116–31.
[35] Tamm I, Kornblau SM, Segall H, Krajewski S, Welsh K, Kitada S, Scudiero DA, Tudor G, Qui YH, Monks A, Andreeff M, Reed JC. Expression and prognostic significance of IAP-family genes in human cancers and myeloid leukemias. Clin Cancer Res 2000;6:1796–803.
[36] Puthalakath H, Strasser A. Keeping killers on a tight leash: transcriptional and post-translational control of the pro-apoptotic activity of BH3-only proteins. Cell Death Differ 2002;9:505–12.
[37] Cheng EH-YA, Wei MC, Weiler S, Flavell RA, Mak TW, Lindsten T, Korsmeyer SJ. BCL-2, BCL-X_L sequester BH3 domain-only molecules preventing BAX- and BAK-mediated mitochondrial apoptosis. Mol Cell 2001;8:705–11.
[38] Bailey SM, Wyatt MD, Friedlos F, Hartley JA, Knox RJ, Lewis AD, Workman P. Involvement of DT-diaphorase (EC 1.6.99.2) in the DNA cross-linking and sequence selectivity of the bioreductive anti-tumor agent EO9. Br J Cancer 1997;76:1596–603.
[39] O'Connor PM, Jackman J, Bae I, Myers TG, Fan S, Mutoh M, Scudiero DA, Monks A, Sausville EA, Weinstein JN, Friend S, Fornace Jr A, Kohn KW. Characterization of the p53 tumor suppressor pathway in cell lines of the National Cancer Institute Anticancer Drug Screen and correlations with the growth-inhibitory potency of 123 anticancer agents. Cancer Res 1997;57:4285–300.
[40] Powis G. Metabolism and reactions of quinoid anticancer agents. Pharmacol Ther 1987;35:57–162.
[41] Gutierrez PL. The metabolism of quinone-containing alkylating agents: free radical production and measurement. Front Biosci 2000;5:629–38.
[42] Mossoba MM, Alizadeh M, Gutierrez PL. Mechanism for the reductive activation of diaziquone. J Pharm Sci 1985;74:1249–54.
[43] Tudor G, Aguilera A, Halverson DO, Laing ND, Sausville EA. Susceptibility to drug-induced apoptosis correlates with differential modulation of BAD, Bcl-2 and Bcl-xL protein levels. Cell Death Differ 2000;7:574–86.
[44] Sun X, Ross D. Quinone-induced apoptosis in human colon adenocarcinoma cells via DT-diaphorase mediated bioactivation. Chem Biol Interact 1996;100:267–76.
[45] Reed CJ. Apoptosis and cancer: strategies for integrating programmed cell death. Semin Hematol 2000;37:9–16.
[46] Tang DG, Li L, Zhu Z, Joshi B. Apoptosis in the absence of cytochrome *c* accumulation in the cytosol. Biochem Biophys Res Commun 1998;242:380–4.
[47] Chauhan D, Hideshima T, Rosen S, Reed JC, Kharbanda S, Anderson KC. Apaf-1/cytochrome-*c* independent and Smac-dependent induction of apoptosis in multiple myeloma (MM) cells. J Biol Chem 2001;276:24453–6.
[48] Pritsos CA, Vimalachandra B. Mitochondrial dysfunction and ATP depletion in mitomycin C treated mice. Proc Am Assoc Cancer Res 1995;36:352–6.